Hindawi
International Journal of Antennas and Propagation
Volume 2023, Article ID 5462081, 13 pages
https://doi.org/10.1155/2023/5462081

Research Article

An Indoor Unknown Radio Emitter Positioning Approach Using Improved RSSD Location Fingerprinting

Liyang Zhang,[1] **Kunlei Liu**,[1] **Zhiyou Pan**,[2] **Lei Pan**,[1] **Rui Gao**,[1] **and Qian Zhang**[1]

[1]*School of Control and Mechanical Engineering, Tianjin Chengjian University, Tianjin 300384, China*
[2]*CATARC Automotive Industry Engineering (Tianjin) Co. Ltd., Tianjin 300300, China*

Correspondence should be addressed to Lei Pan; panlei4089@163.com

Received 27 October 2022; Revised 13 February 2023; Accepted 15 February 2023; Published 28 February 2023

Academic Editor: Khaled Rouabah

The accurate location of an unknown radio emitter (URE) is a critical task in wireless communication security. The URE localization method based on the received signal strength difference (RSSD) has become popular due to the identification of unknown transmitting power and frequency. However, high computational complexity and low positioning accuracy have been caused by the RSSD fingerprint data's redundancy and cross-correlation. In this article, an indoor RSSD-based positioning algorithm combining principal component analysis (PCA) and Pearson correlation coefficient (PCC), called RSSD-PCA-PCC, is proposed to realize efficient feature extraction and reduce false fingerprint matching. Firstly, to achieve reduction and decorrelation, the principal components of the RSSD fingerprint database are extracted by the singular value decomposition (SVD) method. Secondly, the PCC is applied to measure the relative distance between the principal component features. In particular, the PCC is used for selecting the reference points (RPs) in order to match the position accurately. The results show that the proposed algorithm can obtain a more superior performance compared with the conventional RSSD-based weighted k-nearest neighbor algorithm (RSSD-WKNN) and COS matching algorithm (RSSD-PCA-COS) in the case of different selected RP numbers, AP numbers, and grid distances.

1. Introduction

Currently, the indoor location-based service has received great attention with the growth of communication security requirements [1]. Many important fields and occasions such as conference venue, gymnasium, hospital, and shopping mall have been provided with indoor location-based service [2, 3]. In the era of Internet of Things (IoT) [4], the privacy of individuals, enterprises, and even countries has been frequently leaked by the unknown radio emitter (URE). The URE has the risk of illegally occupying wireless communication channels. Thus, accurately locating the URE is crucial to improve the communication security and ensure the confidentiality and integrity of communicating data.

The demand for the indoor positioning service in the commercial and military fields has spawned many positioning techniques and systems. However, the global positioning system (GPS) [5] and the BeiDou navigation satellite system [6] are limited by the scattering and reflection of satellite signals in the complex indoor environments. The satellite positioning technique cannot provide a full coverage indoor location. The dynamic indoor structure, variable layout, and diverse signal band can generate signal multipath reflection and irregular attenuation. At present, the wireless local area network (WLAN), Bluetooth, ultra-wideband (UWB), radio frequency identification (RFID) [7], infrared, and ultrasonic [8] are commonly used methods for indoor positioning. Positioning feature parameters can be divided into two categories depending on whether distance-based measurement parameters are used. Typical localization algorithms based on measured distance are time of arrival (TOA) [9] and time difference of arrival (TDOA) [10]. The ToA parameter can be converted to distance. However, high-precision time

synchronization between the radio emitter and access points (AP) cannot be achieved in the complex multipath indoor environment. The signal receiver is considered an AP. Although TDOA can eliminate clock errors through differential operation, dedicated hardware is still required. Both TOA and TDOA produce measurement errors easily in the non-line-of-sight (NLOS) indoor environment [11]. Angle of arrival (AOA) [12] and received signal strength (RSS) are commonly applied to the positioning feature parameters without distance measurement. Since AOA requires to measure angle by array antenna, the hardware cost and computational complexity increase greatly. RSS has become a research focus due to the unnecessary condition of harsh time synchronization and expensive hardware equipment. However, under the same location and temporal interval condition, the RSS were discrepant due to the different power and antenna gain of the radio emitters [13]. Hence, establishing different RSS fingerprint databases for the radio emitter with different transmitting powers and frequencies would greatly increase workload. Therefore, RSS is not suitable for locating the URE.

A robust location fingerprint called received signal strength difference (RSSD) was derived in the presence of hardware heterogeneity [14]. Since RSSD-based fingerprint positioning techniques have undergone a difference operation of RSS among APs, the power and antenna gain parameters of the radio emitter can be eliminated. Compared with RSS, RSSD-based fingerprint positioning methods not only have stronger stability for heterogeneous emitters but can also realize locating the URE. A new whitened model for RSSD-based localization with unknown transmitting power was presented in [15]. However, the stability of the novel model under multipath effects has not been investigated. A robust two-stage estimator was proposed to locate an URE in the presence of Gaussian mixture measurement noise [16]. Due to the nonlinear problem, the experimental results had significant bias and poor efficiency. In [17], an approach based on RSSD was presented to locate an URE under the condition of sensor position errors. Due to the cost function's high sensitivity to outliers, the performance was easily affected by Gaussian noise in an NLOS environment. In [18], aiming at Gaussian mixture noise in wireless sensor networks, a robust fault-tolerant localization technique (RFLT) based on RSSD was proposed. The problem was nonconvex, and the large residual error was caused by the noise and faulty nodes.

The RSSD fingerprint positioning technique contains offline database establishment and online matching stages. The unprocessed RSSD fingerprint database collected directly by receivers is redundant and inaccurate due to complex signal interference. Database deviation break the one-to-one mapping relation between the geometric coordinate and RSSD measurement. A number of improved methods have been proposed to solve the problem of related redundancy in the RSS-based database and significantly improve positioning accuracy. Common approaches to solve the curse of the dimensionality problem can be divided into two categories: one is to select a suitable subset of APs, and the other is to project RSS into an alternative space. Only partial APs adopted can ignore useful information [19, 20]. Hence, data projection is a more efficient information compaction approach. Through projecting the measured signal into a decorrelated signal space, the linear combination of all APs can be obtained. The principal component analysis (PCA) with low complexity and cost has been widely employed in the positioning algorithms. A variety of approaches using the Nearest Neighbor (NN), K-Nearest Neighbor (KNN), and weighted K-Nearest Neighbor (WKNN) algorithms combined with RSS-PCA feature extraction have been proposed for the indoor positioning system [21, 22]. In [21], PCA was utilized to improve the performance and reduce the computation cost of the WiFi indoor positioning systems based on machine learning approaches such as Support Vector Machines (SVM), KNN, Decision Trees (DTs), and Random Forest (RF). The PCA dealt with the high dimensionality radio map by using a covariance matrix to map the features into an uncorrelated space. And the Euclidean distance was used to calculate the distance between features at the online stage. In order to reduce the dimension of RSS and remove the noisy measurements, the PCA method was applied over all clustered RPs [23]. Then, similarity matching algorithms such as Cosine similarity (COS), Pearson correlation coefficient (PCC), and Tanimoto similarity were tested by applying the offline fingerprint database. The COS and PCC achieved the same accuracy. The Tanimoto similarity obtained the higher accuracy in recognizing the suitable cluster. However, the matching accuracy of COS and PCC in the online stage was not tested. A hierarchical localization method was proposed in [22], and PCA was applied on each subset to perform feature extraction. Then, position estimation was acquired by WKNN. Localization performance of Euclidean distance, COS, PCC, and Manhattan distance was verified over different K values. The COS and PCC provided better performance than the other two similarity functions, while the difference between PCC and COS was deficient. The COS was chosen due to the easier computation. Nevertheless, the positioning accuracy is not high in the results. In summary, the above references all combine the RSS fingerprint with the PCA method for the indoor positioning system. In this article, RSSD is utilized as the locating feature in order to realize the positioning of the URE. The RSSD has higher data redundancy and computational complexity than RSS. Processing the RSSD fingerprint database by PCA in advance is necessary to reduce the positioning error. Specifically, this article applies singular value decomposition (SVD) to extract the principal component according to RSSD matrix singularity. The SVD can directly perform singular value decomposition on arbitrary matrices without covariance matrix calculation. A technique based on SVD and multidimensional scaling (MDS) [24] was presented to verify the optimality of the SVD-reconstruct approach.

The fingerprint matching method is the key step to achieve higher positioning accuracy after offline database processing. Distance measurements or similarity functions can be used to measure similarity among databases [25]. Based on the conventional absolute distance measurement methods such as Euclidean distance and Manhattan distance, the WKNN can obtain better positioning performance than NN and KNN by weighting the positions of

reference points (RPs). In order to meet the requirement of the RSS calibration for different kinds of Bluetooth devices, RSSD and distance ratio were used as localization characteristic parameters [26]. And various positioning algorithms based on Euclidean distance were discussed such as NN, KNN, multistep, and nonlinear optimization. In [27], the Manhattan distance was used in the WKNN algorithm to improve positioning accuracy. However, the conventional absolute distance can only measure a sample with the same dimension. The principal component database processed by PCA has eliminated the dimensional influence among the features. Conventional absolute distance such as Euclidean distance or Manhattan distance cannot measure similarity between offline and online principal component databases. Some fingerprint matching algorithms based on probability usually require probabilistic assumptions and more datasets than conventional deterministic algorithms [28]. The COS and PCC are common similarity functions to measure relative distance. References [29] simulate dense fingerprints while exploring the COS of the directions to WiFi access APs. Due to the fact that the COS only spots the differences from the vector direction, errors in localization results are generated when the target and chosen RPs are on the same line. In [30], adjusted cosine similarity (ACS) was employed in the online stage to solve the issue of outliers produced by cosine similarity. The PCC normalizes the data and solves the COS deficiencies by focusing on the vector direction and ignoring the absolute value. In this article, an indoor localization algorithm that combines PCA and PCC, called RSSD-PCA-PCC, is proposed to improve the positioning accuracy of an URE. The PCC has superiority in measuring the similarity of the principal component database. The PCC is often used for classification and regression prediction. In [31], an algorithm based on the PCC was used to accurately determine time of flight (TOF) of signals scattered by the object. A fusion indoor positioning system [32] that combined dynamic time warping (DTW) and PCC was designed to find observation corner coordinates. A regional division and AP optimization algorithm was employed in [33] to solve the problem of low positioning efficiency caused by the redundant RSS database. The WKNN algorithm combined with the PCC matching method was utilized to locate the target in the online positioning stage. However, the single RSS feature parameter has limitations in locating the URE. The above references have few comparative analyses of PCC and COS matching methods in the online stage. In this article, considering the complexity and accuracy of the location estimation, the RSSD measurement is projected into an uncorrelated subspace and the PCC is used to evaluate the similarity of RSSD principal component databases between offline and online stages. In addition, compared with COS, the superiority of the PCC can be verified under the same conditions. The proposed RSSD-PCA-PCC algorithm is described in the following section:

In order to achieve the accurate localization of an URE, this article is devoted to the improvement of the fingerprint database and the matching algorithm. The contributions of this article are as follows:

(1) In order to reduce the database dimension and eliminate the RSSD correlation, a feature extraction method based on PCA is proposed to project the RSSD fingerprint database into a subspace. Both offline and online RSSD principal component databases can be obtained by SVD.

(2) A fingerprinting matching approach using the PCC is designed to determine the similarity and select RP reasonably. Thus, the RSSD-PCA-PCC algorithm is proposed to eliminate inherent drawbacks of the RSSD fingerprint database and reduce false matching.

(3) The advantages of the proposed algorithm are verified by comparing it with the RSSD-WKNN and RSSD-PCA-COS algorithms under the conditions of different RP numbers, AP numbers, and grid distances.

The remainder of this article is organized as follows: Section 2 presents the theory related to the PCA, the PCC, and the designed system model. The proposed database feature extraction method based on SVD and the PCC fingerprint matching process are depicted in Section 3. Section 4 provides validation results, analysis, and comparisons. Conclusions are given in Section 5.

2. The Principle and System Model

In this section, the function and solution procedures for PCA and PCC are presented specifically. Then, the indoor URE positioning system based on the RSSD-PCA-PCC is established and presented.

2.1. Principal Component Analysis. PCA is the most classic and widely used reduced-dimension method based on eigenvector analysis. By the orthogonal similarity transformations, a set of vectors is selected in the sample space as a projection matrix. Through projection, the high-dimensional data are mapped into the low-dimensional space. Using fewer data dimensions can retain the more dominant features of the original data. The key task of feature extraction is to access appropriate transformations. The most commonly used transformation method is linear transformation. If $x \in \mathbb{R}^D$ is the D-dimensional primitive feature matrix, the transformed d-dimensional decorrelation feature $\xi \in \mathbb{R}^d$ is: $= W^T x$, where W is the $D \times d$-dimensional transformation matrix called the projection matrix.

There are two common methods to receive the projection matrix in PCA: one is eigenvalue decomposition (EVD), and the other is singular value decomposition (SVD). The database containing all samples is represented as a matrix $A \in \mathbb{R}^{m \times m}$. According to the basic theory of EVD, a formula can be expressed as follows:

$$Av = \lambda v, \tag{1}$$

where λ is the eigenvalue in descending order and v is the corresponding eigenvector. Then, A can be decomposed into

$$A = Q_i \Lambda_{ii} Q_i^{-1}, i = 1, \cdots, m, \tag{2}$$

where Q_i corresponds to the *i-th* column of v and Λ_{ii} is eigenvalue matrix satisfying $\Lambda_{ii} = \lambda_i$. EVD is suitable for the nonsingular matrix. However, the constructed RSSD fingerprint data matrix is not a square matrix. SVD is suitable for the decomposition of arbitrary matrices. The principle of SVD is discussed in detail as follows.

A singular matrix $B \in \mathbb{R}^{m \times n}$ is given, where m represents sampling numbers and n is the number of features contained in each sample. Then, orthogonal matrices $U \in \mathbb{R}^{m \times m}$ and $V \in \mathbb{R}^{n \times n}$ can be defined as follows:

$$B = U \Sigma V^T, \tag{3}$$

where $\Sigma = \begin{bmatrix} \Sigma_1 & O \\ O & O \end{bmatrix}$ and $\Sigma_1 = \text{diag}(\sigma_1, \sigma_2, \ldots, \sigma_r)$. The diagonal elements are arranged in descending order.

$$\sigma_1 \geq \sigma_2 \geq \cdots \geq \sigma_r > 0, r = \text{rank}(B), \tag{4}$$

where values $\sigma_1, \sigma_2, \ldots, \sigma_r$ and $\sigma_{r+1} = \sigma_{r+2} = \ldots = \sigma_{\min\{m,n\}} = 0$ are called singular values of the matrix B together. In particular, a proven mathematical relationship between the singular value and the eigenvalue can be established as follows:

$$\Sigma_1 = \sqrt{\Lambda_1}, \tag{5}$$

where Λ_1 is the eigenvalue matrix of $B^T B$. The explanations about singular vectors are as follows

The Vright-multiplying formula (3) can be expressed as follows:

$$BV = U\Sigma. \tag{6}$$

The column vector form can be represented as follows:

$$Bv_i = \begin{cases} \sigma_i u_i, i = 1, 2, \cdots, r, \\ 0, i = r+1, r+2, \cdots, \min\{m, n\}, \end{cases} \tag{7}$$

where the column vector v_i of V is called the right singular vector of B and V is called the right singular vector matrix. The first r columns of V form the orthonormal basis of the matrix B row space.

The U^Hleft-multiplying formula (3) can be expressed as follows:

$$U^H B = \Sigma V^T. \tag{8}$$

The column vector form can be represented as follows:

$$u_i^H B = \begin{cases} \sigma_i v_i^T, i = 1, 2, \cdots, r, \\ 0, i = r+1, r+2, \cdots, \min\{m, n\}, \end{cases} \tag{9}$$

where the column vector u_i of U is called the left singular vector of B and U is called the left singular vector matrix. The first r columns of U form the orthonormal basis of the matrix B column space. The SVD vector form of B can be expressed as follows:

$$B = \sum_{i=1}^{r} \sigma_i u_i v_i^H. \tag{10}$$

When the rank of B satisfies $r = \text{rank}(B) < \min\{m, n\}$ and singular values $\sigma_{r+1} = \ldots = \sigma_h = 0, h = \min\{m, n\}$, formula (3) can be simplified to the truncated SVD expressed as follows:

$$B = U_r \Sigma_r V_r^H, \tag{11}$$

where $U_r = [u_1, u_2, \ldots, u_r]$, $V_r = [v_1, v_2, \ldots, v_r]$, and $\Sigma_r = \text{diag}(\sigma_1, \sigma_2, \ldots, \sigma_r)$, and the number of nonzero singular values r and the corresponding values $\sigma_1, \sigma_2, \ldots, \sigma_r$ are uniquely determined relative to the matrix B.

To achieve data reduced-dimension, the essence of SVD is to choose main dimension of data distribution and map original high-dimensional data into a low-dimensional subspace. Considering the linear independence among the features after projection, both v_i and u_i obtained by SVD are unitary matrices. Each singular vector can be regarded as a projection surface. And the corresponding singular value represents the variance after projection. According to the maximum variance theory, the larger variance contains the more information. Therefore, the singular vectors with larger singular values should be selected to form the projection surface. The projection matrix can be expressed as follows:

$$P = [p_1, p_2, \cdots, p_a]^T, a < r. \tag{12}$$

Then, P is used to project the original sample matrix into the subspace. The principal component matrix after dimension reduction and RSSD decorrelation can be received.

2.2. Pearson Correlation Coefficient. In statistics, the PCC is applied to measure the degree of correlation between two variables. And the value ranges from −1 to +1. The larger the absolute value of the coefficient, the higher the correlation between X and Y. The PCC is defined as the quotient of the covariance and standard deviation between the two variables. According to unbiased estimates in statistics, the variance can be calculated as follows:

$$\sigma_X^2 = D(X) = \frac{\sum_{i=1}^{N} (X_i - \mu)^2}{N - 1}, \tag{13}$$

where N is data quantity and $\mu = \overline{X}$ is overall mean. The standard deviation σ_X can intuitively reflect the dispersion degree of the database. Variance can measure the change tendency of a single random variable, while covariance can describe the change degree of two different random variables. The formula for covariance is given as follows:

$$Cov(X, Y) = E[(X - E[X])(Y - E[Y])], \tag{14}$$

where E stands for mathematical expectation. The PCC derivation process can be obtained as follows:

$$\rho_{XY} = \frac{Cov(X,Y)}{\sigma_X \sigma_Y} = \frac{E[(X - E[X])(Y - E[Y])]}{\sqrt{D(X)}\sqrt{D(Y)}} = \frac{\sum_{i=1}^{n}(X_i - \overline{X}) \cdot (Y_i - \overline{Y})}{\sqrt{\sum_{i=1}^{n}(X_i - \overline{X})^2} \cdot \sqrt{\sum_{i=1}^{n}(Y_i - \overline{Y})^2}}. \quad (15)$$

For equation (15), the first equality comes from the definition of the PCC, the second equality is based on the formulas (13) and (14), and the last equality is often used for actual operation. The corresponding relation between different ρ absolute values and correlative degrees is described in Table 1.

2.3. System Model. The typical indoor fingerprint positioning system involves the offline and online stages. The fundamental purpose of the offline stage is to integrate the geometric coordinate and the RSSD of each RP. Then, the fingerprint database with the location label can be constructed. In the online stage, the RSS of target can be measured. And the estimated coordinate can be obtained by the appropriate matching algorithm. The purpose of this article is to accurately locate an URE. Comparing with the conventional fingerprint-based indoor positioning system, this article makes improvements in both offline and online stages. Figure 1 shows the proposed RSSD-PCA-PCC positioning system structure.

In the offline stage, appropriate grid distance should be selected to divide into subpositioning areas. Each vertex can be regarded as an RP. In our system, four APs are uniformly applied as an example. The known radio emitter is placed at each RP in turn. Then, the RSS measurements are collected at each AP. Each RP corresponds to a set of specific location fingerprint vectors and represents the unique scene characteristics. The RP coordinates and the difference between AP observations make up the offline RSSD database. However, the RSSD of each adjacent calculation has a high spatial and temporal correlation. In this article, a more efficient information compaction method based on PCA illustrated with red colour is applied to reduce online computational complexity and improve positioning accuracy. The projection matrix can be obtained by using the SVD decomposition method. The detailed procedures are expressed in the next section.

In the online stage, real-time RSS from the URE can be received by APs. Then, the online RSSD database can be achieved by difference operation. Dimension reduction and RSSD decorrelation processing are completed by the projection matrix. The focus of the online positioning stage is to find the most closely related RP combinations. As shown in Figure 1, the similarity can be evaluated by calculating the PCC (marked with green). The calculation results are denoted by ρ and sorted in descending order. Finally, the RP coordinates can be selected to estimate the URE position.

3. Proposed RSSD-PCA-PCC Positioning Algorithm

In this section, detailed procedures of the proposed RSSD-PCA-PCC positioning system are introduced to estimate the location of an URE.

Table 1: Correlative degree for different ρ absolute values.

ρ	Correlative degree
0.8 ~ 1.0	Very strong correlation
0.6 ~ 0.8	Strong correlation
0.4 ~ 0.6	Moderate correlation
0.2 ~ 0.4	Weak correlation
0.0 ~ 0.2	Very weak or no correlation

3.1. RSSD-Based Database Reconstruction. Assuming that there are L RPs and M APs in the positioning area, the offline RSS fingerprint database is shown in Table 2.

The RSS measurements received by different APs can be considered as multiple dimensions. Thus, each RP has multidimensional fingerprint features. The offline RSSD fingerprint database is shown in Table 3.

Each row in the Table 3 represents a sample and each column represents an original feature. Thus, each RP has $\complement_M^2$ features. Extracting principal components from multiple dimensions can result in a more robust fingerprint database. In this article, PCA is used to reduce the feature space dimensions and eliminate correlation among original features. The offline RSSD sample matrix is given as follows:

$$RSSD = \begin{bmatrix} RSSD_{1,1-2} & RSSD_{1,2-3} & \cdots & RSSD_{1,M-1} \\ RSSD_{2,1-2} & RSSD_{2,2-3} & \cdots & RSSD_{2,M-1} \\ \vdots & \vdots & \vdots & \vdots \\ RSSD_{L,1-2} & RSSD_{L,2-3} & \cdots & RSSD_{L,M-1} \end{bmatrix}. \quad (16)$$

Due to the singularity of the RSSD matrix, SVD is chosen as the specific implementation method of PCA. The SVD theory has proven that RSSD can be decomposed into the following formula:

$$RSSD = USV^T, \quad (17)$$

where the detailed derivation processes of U, V, and S are deduced in the following.

Firstly, the transpose matrix $RSSD^T$ can be achieved, and then the $RSSD_1^*$ can be expressed as follows:

$$RSSD_1^* = \left(RSSD^T\right)(RSSD) = \begin{bmatrix} R_{1,1} & \cdots & R_{1,\complement_M^2} \\ \vdots & \vdots & \vdots \\ R_{\complement_M^2,1} & \cdots & R_{\complement_M^2,\complement_M^2} \end{bmatrix}. \quad (18)$$

The eigenvalue λ_1^* and the eigenvector μ of $RSSD_1^*$ can be calculated. Then, λ_1^* can be sorted in descending order. The corresponding eigenvector can be stored to form the matrix $E_{1_{\complement_M^2 \times \complement_M^2}}$.

$$\lambda_1^* = \left[\lambda_1, \lambda_2, \cdots, \lambda_{\complement_M^2}\right], \quad E_1 = \left[e_1, e_2, \cdots, e_{\complement_M^2}\right]. \quad (19)$$

The equation between E_1 and the right singular vector V can be expressed as follows:

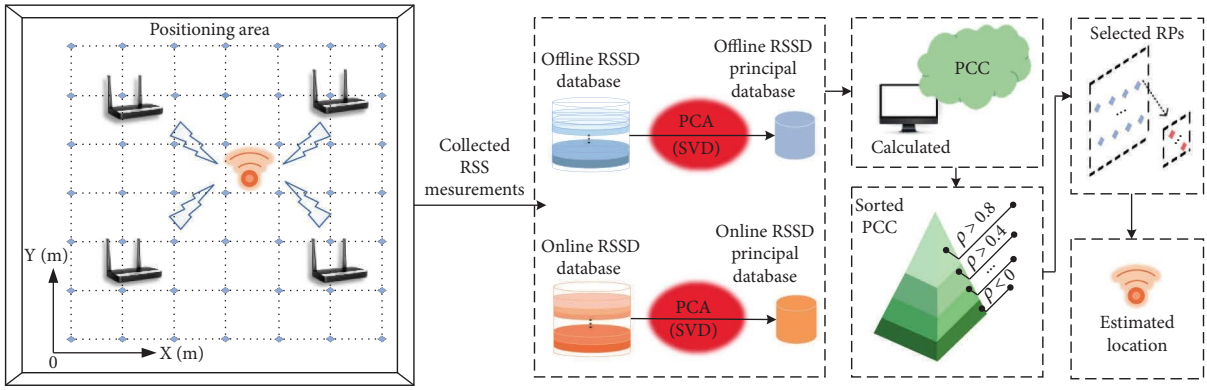

Figure 1: The structure of the proposed RSSD-PCA-PCC positioning system.

Table 2: The offline RSS fingerprint database.

Coordinates	RSS sample			
(x_1, y_1)	$RSS_{1,1}$	$RSS_{1,2}$	...	$RSS_{1,M}$
(x_2, y_2)	$RSS_{2,1}$	$RSS_{2,2}$	...	$RSS_{2,M}$
(x_3, y_3)	$RSS_{3,1}$	$RSS_{3,2}$	...	$RSS_{3,M}$
⋮	⋮	⋮	⋮	⋮
(x_L, y_L)	$RSS_{L,1}$	$RSS_{L,2}$	...	$RSS_{L,M}$

Table 3: The offline RSSD fingerprint database.

Coordinates	RSSD sample			
(x_1, y_1)	$RSSD_{1,1-2}$	$RSSD_{1,2-3}$	...	$RSSD_{1,M-1}$
(x_2, y_2)	$RSSD_{2,1-2}$	$RSSD_{2,2-3}$	...	$RSSD_{2,M-1}$
(x_3, y_3)	$RSSD_{3,1-2}$	$RSSD_{3,2-3}$	...	$RSSD_{3,M-1}$
⋮	⋮	⋮	⋮	⋮
(x_L, y_L)	$RSSD_{L,1-2}$	$RSSD_{L,2-3}$	...	$RSSD_{L,M-1}$

$$V = E_1. \tag{20}$$

According to mathematical relationship between the eigenvalue and the singular value, the singular value matrix S can be obtained as follows:

$$S_i = \sqrt{\lambda_i}, i = 1, 2, \cdots, \complement_M^2. \tag{21}$$

The calculation process of the left singular matrix U is similar to V. The $RSSD_2^*$ can be expressed as follows:

$$RSSD_2^* = (RSSD)\left(RSSD^T\right) = \begin{bmatrix} R_{1,1} & \cdots & R_{1,L} \\ \vdots & \vdots & \vdots \\ R_{L,1} & \cdots & R_{L,L} \end{bmatrix}. \tag{22}$$

Similarly, the eigenvalue λ_2^* and the eigenvector E_2 of $RSSD_2^*$ are obtained by the feature decomposition method. Then, $U = E_2$ can be achieved.

The first a columns of V is extracted to form the projection matrix $P_{\complement_M^2 \times a}$. The principal component matrix Z_1 can be expressed as follows:

$$Z_{1_{L \times a}} = RSSD \cdot P. \tag{23}$$

Then, the offline principal component fingerprint database $PRSSD^*$ can be obtained as follows:

$$PRSSD^* = \begin{bmatrix} prssd_1^*, (x_1, y_1) \\ prssd_2^*, (x_2, y_2) \\ prssd_3^*, (x_3, y_3) \\ \vdots \\ prssd_L^*, (x_L, y_L) \end{bmatrix}, \tag{24}$$

where each row is a principal component matrix with a-dimensional linearly independent features. $prssd_1^*$ can be described as follows:

$$prssd_1^* = \left[prssd_{1,1}; prssd_{1,2}; \cdots; prssd_{1,a}\right]. \tag{25}$$

Due to $a < \complement_M^2$, the size of the database can be greatly reduced in the decorrelated space. In addition, the online fingerprint matching stage has lower computational complexity. The dimension reduction and decorrelation processing of the RSSD offline fingerprint database are realized. When the target enters the test area, the RSS real-time measurement results of all APs can be obtained. The unprocessed RSSD online fingerprint database is obtained by differential operation. Similarly, P is used to project the RSSD online fingerprint database into the subspace. The dimension reduction and RSSD decorrelation processing can be expressed as follows:

$$Z_2 = \widetilde{RSSD} \cdot P, \tag{26}$$

where $\widetilde{RSSD}$ is the online RSSD sample matrix. The online principal component fingerprint database $P\widetilde{RSSD}^*$ can be obtained as follows:

$$P\widetilde{RSSD}^* = \left[prssd_1, prssd_2, \cdots, prssd_a\right]. \tag{27}$$

The database with the most indispensable fingerprint features has been extracted. However, conventional absolute distance such as Euclidean distance cannot measure similarity between offline and online principal component databases. In this article, a matching algorithm based on similarity called the PCC is applied to replace the distance measurement method.

3.2. Location Calculation Process. The indoor fingerprint positioning algorithm needs to develop reasonable matching

methods to ensure accuracy. The PCC method can identify the similarity among dimensionless samples. For offline and online principal component fingerprint databases, the PCC can be calculated as follows:

$$\rho\left(PRSSD^*, \widetilde{PRSSD}^*\right) = \rho(\alpha,\beta) = \frac{Cov(\alpha,\beta)}{\sigma_\alpha \cdot \sigma_\beta} = \frac{\sum_{i=1}^{a}(\alpha_i - \overline{\alpha})\cdot(\beta_i - \overline{\beta})}{\sqrt{\sum_{i=1}^{a}(\alpha_i - \overline{\alpha})^2}\cdot\sqrt{\sum_{i=1}^{a}(\beta_i - \overline{\beta})^2}}, \tag{28}$$

where α and β stand for $PRSSD^*$ and $\widetilde{PRSSD}^*$, respectively. $\overline{\alpha}$ and $\overline{\beta}$ are the mean values. σ_α and σ_β represent the standard deviations. The PCC between the URE and all RPs can be obtained through formula (28). The RP coordinates with the largest coefficients are selected for position estimation. The estimated coordinate (x_{URE}, y_{URE}) can be obtained by the RSSD-PCA-PCC algorithm.

$$\begin{cases} x_{URE} = \dfrac{1}{K}\displaystyle\sum_{i=1}^{K} x_i \\ y_{URE} = \dfrac{1}{K}\displaystyle\sum_{i=1}^{K} y_i, \end{cases} \tag{29}$$

where (x_i, y_i) represents the coordinate of the $i\text{-}th$ RP and K is the number of selected RPs. Combining with the PCC matching method, the RPs can be selected based on the KNN approach [34] and the performance of different K values chosen by the PCC has been explored in this article.

The procedure of the proposed RSSD-PCA-PCC positioning system is shown in Figure 2. The blue and orange boxes represent the principal component extraction process of offline and online RSSD fingerprint databases, respectively. The green frame represents the process of calculating the PCC for fingerprint matching. The performance evaluations of the proposed RSSD-PCA-PCC algorithm are described in the next section. The proposed RSSD-PCA-PCC algorithm is summarized in Table 4.

4. Results and Analysis

4.1. Positioning Performances. In this article, the average error (AE), root mean square error (RMSE), and computational complexity are used as three key indicators to validate the localization performance of the proposed RSSD-PCA-PCC algorithm. A typical easy-to-implementlog-normal shading model [35] is used to generate the RSS under an indoor environment, which can be explained as follows:

$$P\left(d_{p,q}\right) = P(d_0) - 10\cdot\alpha\cdot\log\left(\frac{d_{p,q}}{d_0}\right) + \chi_q, \tag{30}$$

where $d_{p,q}$ represents the distance between $p\text{-}th$ AP and $q\text{-}th$ RP, $P(d_{p,q})$ is the RSS of $q\text{-}th$ RP at distance $d_{p,q}$ from $p\text{-}th$ AP, d_0 is the reference distance, and $P(d_0)$ is the RSS of the reference distance. α is the path loss index and χ_q is a Gaussian random noise obey $(0, \sigma^2)$. σ^2 represents the measurement variance of RSS. The parameters of equation (30) are set as done in reference [35]. $P(d_0)$ is relevant to the transmit power. The heterogeneous emitters usually have different $P(d_0)$. The offline RSS and RSSD databases are established as done in [35]. Then, the RSS-WKNN and RSSD-WKNN algorithms are utilized to demonstrate the applicability of RSSD for locating the URE. And the AE comparison is shown in Figure 3. The available positioning accuracy of RSS only occurs occasionally when $P(d_0)$ of the offline and online stages is same. In contrast, RSSD is able to maintain stable positioning accuracy. Obviously, RSS is not suitable for the localization of the URE. In this article, to effectively compare the positioning performance of the proposed RSSD-PCA-PCC algorithm, the same RSSD database is applied for comparative analysis.

The performance of the proposed RSSD-PCA-PCC algorithm is shown in Figure 4. A 100 m × 100 m positioning area is applied including 150 randomly selected single-target locations marked with $''*''$, four APs identified by solid pentagrams, and the location results using the proposed RSSD-PCA-PCC algorithm marked with solid circles. The APs are arranged in $''N''$ shape, and the locations are (33.2, 75.2) m, (17.2, 25.2) m, (83.2, 75.2) m, and (70.2, 25.2) m, respectively. The RPs are evenly distributed in the positioning area with 2 m grid distance. And the selected RP numbers is denoted by $K = 4$. From Figure 4, the AE and RMSE are only 0.82 m and 0.95 m, respectively.

In order to demonstrate the superiority of the proposed RSSD-PCA-PCC algorithm, RSSD-PCA-COS and RSSD-WKNN methods are utilized to compare the performance. Based on the same propagation model parameters, 100 positioning targets are randomly selected in the 100 m × 100 m positioning area. Figure 5 shows the cumulative distribution function (CDF) of the three algorithms. The CDF reflects probability distribution of different location error ranges. According to the CDF curve, the RSSD-PCA-PCC has the 2 m location error at a probability of 0.88. Under the same location error, the probabilities of RSSD-PCA-COS and RSSD-WKNN are 0.8 and 0.19, respectively. Obviously, the number of qualified positioning results of the RSSD-PCA-PCC is greater than the other two algorithms. Considering the location error within 1 m, the CDF for each algorithm is 58 percent for RSSD-PCA-PCC, 51 percent for RSSD-PCA-COS, and 3 percent for RSSD-WKNN. The results show that the proposed RSSD-PCA-PCC is superior to the other two algorithms in terms of CDF.

A multistacked bar chart is further drawn as shown in Figure 6. According to the size of the area occupied by different colours, the difference in the percentage of different errors can be seen intuitively. The AE of using the proposed RSSD-PCA-PCC algorithm is less than 3 m. The percentage of the RSSD-PCA-PCC with the RMSE greater than 6 m is small. And there is no part with the RMSE greater than 10 m. The RSSD-PCA-PCC has the AE less than 1 m at a percentage of 58%, whereas the percentage at this AE with RSSD-PCA-COS and RSSD-WKNN is 51% and 3%, respectively. The RSSD-PCA-PCC has the RMSE less than 2 m at a percentage of 68%, whereas the percentages at this error with RSSD-PCA-COS and RSSD-WKNN are 67% and 4%, respectively. Both the AE and RMSE of the RSSD-PCA-PCC are superior to the other two localization algorithms.

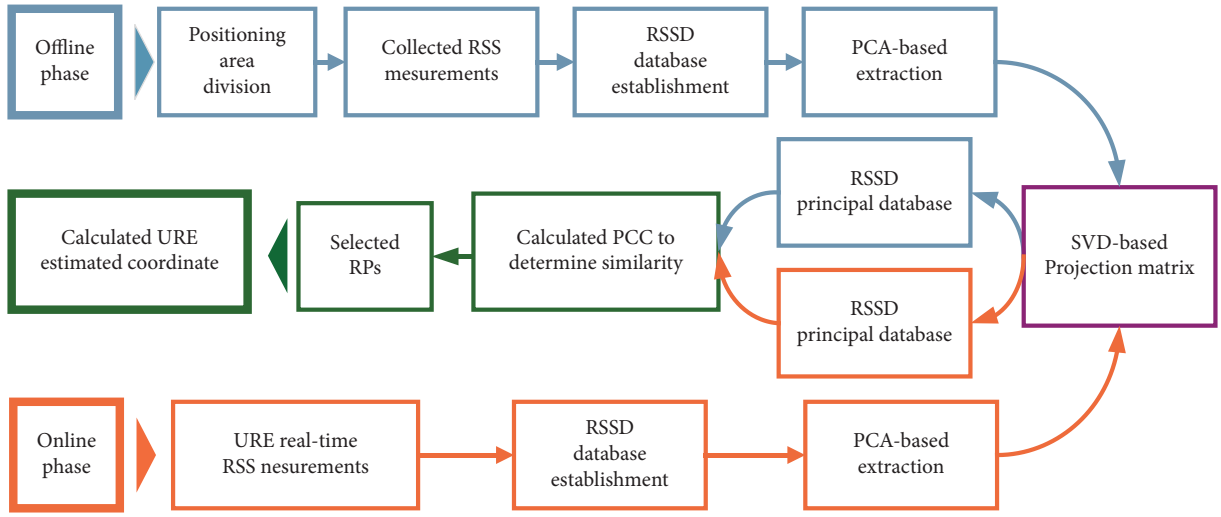

Figure 2: The flowchart of the proposed RSSD-PCA-PCC algorithm.

Table 4: Steps of the proposed RSSD-PCA-PCC algorithm.

Proposed RSSD-PCA-PCC algorithm
(1) Input RSS of L RPs from M APs, calculate the difference of RSS between APs, and build the RSSD offline fingerprint database with known RP coordinates: $[\ (x_l, y_l)\ \ RSSD_{l,N}\ ], l = 1, 2, \cdots, L; N = 1, 2, \cdots, \mathbb{C}_M^2$
(2) Calculate the eigenvalue λ_1^* and the eigenvector μ of $RSSD^* = (RSSD^T)(RSSD)$
(3) Acquire the singular vector V by equation (20)
(4) Extract the first a columns of V to form the projection matrix $P_{\mathbb{C}_M^2 \times a}$
(5) Obtain the offline principal component database $PRSSD^*$ according to equations (23) and (24)
(6) Compute the online database $\widetilde{RSSD}$ of a target by differential operation
(7) Obtain the online principal component database $P\widetilde{RSSD}^*$ according to equations (26) and (27)
(8) Calculate the PCC for offline and online principal component databases using equation (28)
(9) Select RP coordinates with the largest coefficients
(10) Output the estimated coordinate (x_{URE}, y_{URE}) by equation (29)

In addition, this subsection also explored the performance of different selected RP numbers, AP numbers, and grid distances on localization accuracy. Firstly, Figures 7 and 8 compare the AE and RMSE of RSSD-WKNN, RSSD-PCA-COS, and the proposed algorithm RSSD-PCA-PCC under different selected RP numbers, respectively. And the selected RP numbers are denoted by K. Obviously, the positioning accuracy has been significantly improved with the extraction of the principal features. The AE and RMSE of the feature extraction algorithms are less than 2.5 m. By contrast, the RSSD-WKNN algorithm without preprocessing is all higher than 3.5 m under different selected RP numbers. The performance of the RSSD-WKNN algorithm is sequentially inferior to the RSSD-PCA-COS algorithm and the RSSD-PCA-PCC algorithm. When $K = 4$, three algorithms have the lowest AE and RMSE. And the AE and RMSE of the proposed algorithm are stable at 1 m and 1.5 m, respectively. Due to indefinite factors such as random target selection, changing scenes, and complex noise, it is normal for the error curve to fluctuate within a certain range.

Figure 9 presents the error histograms of the three algorithms with different grid distances denoted by d. The heights of the bars represent the errors of different algorithms at different RP grid distances. The proposed algorithm, RSSD-PCA-PCC, has the lowest error under different grid distances. The highest positioning accuracy is obtained when the RP grid distance is 2 m. Taking $d = 2\,m$ as an example, the AE and RMSE of the proposed algorithm RSSD-PCA-PCC are both less than 1 m. As shown in Figure 9, when the grid distance is 0.8 m, the error of RSSD-WKNN is much larger than the error of the other two algorithms. Due to the dense distribution of RPs, the unprocessed database contains a large number of redundant features. False fingerprint matching and high computational complexity affect the positioning accuracy. The database processed by PCA can solve the drawback and obtain the higher positioning accuracy.

Figure 10 shows error histograms of the three positioning algorithms under different AP numbers. When the AP number is three, the AE of the RSSD-PCA-PCC algorithm is 1.68 m. In comparison, the AE of RSSD-WKNN and RSSD-PCA-COS are 2.45 m and 4.63 m, respectively. With the AP number increasing to four, the AE of RSSD-PCA-PCC, RSSD-PCA-COS, and RSSD-WKNN are 0.92 m, 1.28 m, and 3.61 m, respectively. When the AP number is five, the AE and RMSE of the RSSD-PCA-PCC algorithm are smaller than the other two algorithms. By reducing or increasing AP quantities, the proposed algorithm has superior positioning accuracy and stability than RSSD-PCA-PCC and RSSD-WKNN algorithms. From the results in Figure 10, the proposed RSSD-PCA-PCC algorithm can obtain a more superior performance when 4 APs are arranged. With the 4 APs, the RMSE of RSSD-WKNN, RSSD-PCA-COS, and

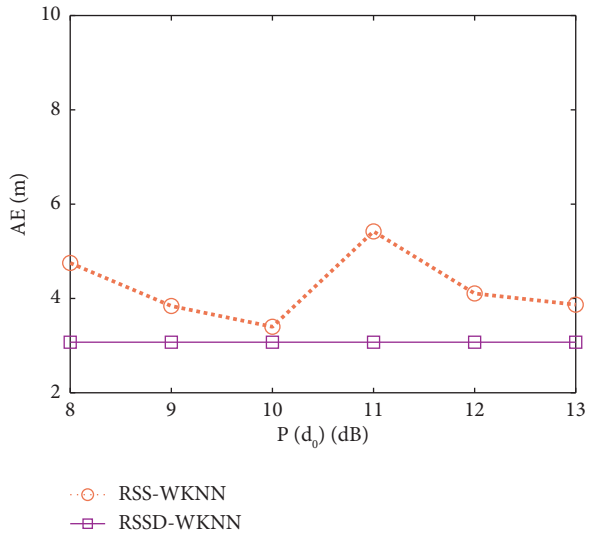

Figure 3: AE comparisons between RSS-WKNN and RSSD-WKNN under different $P(d_0)$ with 2 m grid distance, 4 APs, and $K = 4$.

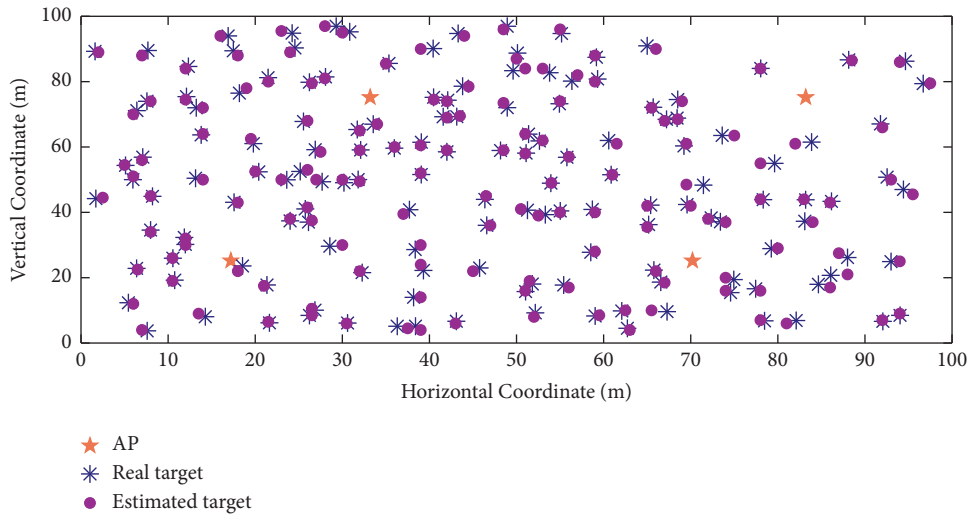

Figure 4: Positioning results of the proposed RSSD-PCA-PCC algorithm with 2 m grid distance, 4 APs, and $K = 4$.

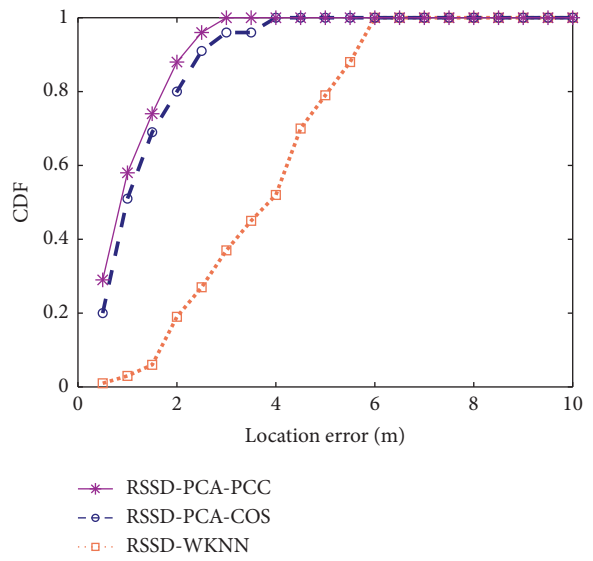

Figure 5: CDF comparisons of location errors among RSSD-WKNN, RSSD-PCA-COS, and proposed RSSD-PCA-PCC with 2 m grid distance, 4 APs, and $K = 4$.

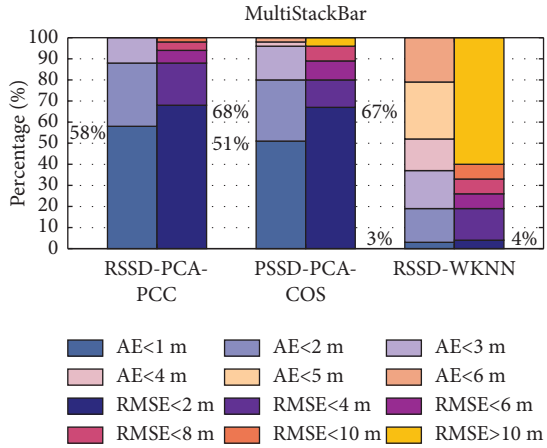

Figure 6: Percentage comparisons of location errors among RSSD-WKNN, RSSD-PCA-COS, and proposed RSSD-PCA-PCC with 2 m grid distance, 4 APs, and $K = 4$.

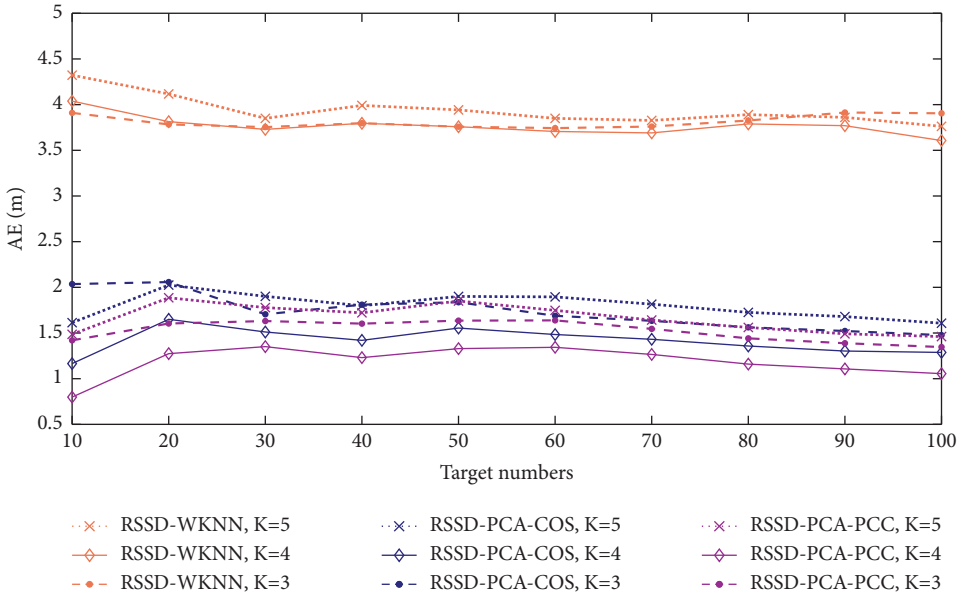

Figure 7: AE comparisons among RSSD-WKNN, RSSD-PCA-COS, and proposed RSSD-PCA-PCC when the number of positioning targets changes from 10 to 100 with 2 m grid distance and 4 APs.

RSSD-PCA-PCC are 3.88 m, 1.62 m, and 1.12 m, respectively. The results prove that the RSSD-PCA-PCC algorithm can realize the precise localization of the URE.

4.2. Computational Complexity. In addition, the computational complexity is also a performance index often considered in the evaluation of an algorithm. The computational complexity of the three different algorithms can be compared and analyzed. Firstly, the computational complexity can be expressed as the number of fingerprints searched in the online stage. Therefore, the computational complexity of RSSD-WKNN is proportional to the number of RPs. It is assumed that the positioning area contains N RPs. After dimension reduction, the principal component database contains n fingerprint features. The computational complexities of RSSD-WKNN and RSSD-PCA-PCC are $O(N)$ and $O(n)$, respectively. Due to $n < N$, the proposed RSSD-PCA-PCC algorithm not only reduces the computational complexity but also decreases the memory space. Secondly, based on the MATLAB2018b platform, the running time of the three different algorithms are compared with 2 m grid distance, 4 APs, $K = 4$, and the same target locations. As shown in Table 5, the proposed RSSD-PCA-PCC algorithm has the shortest running time.

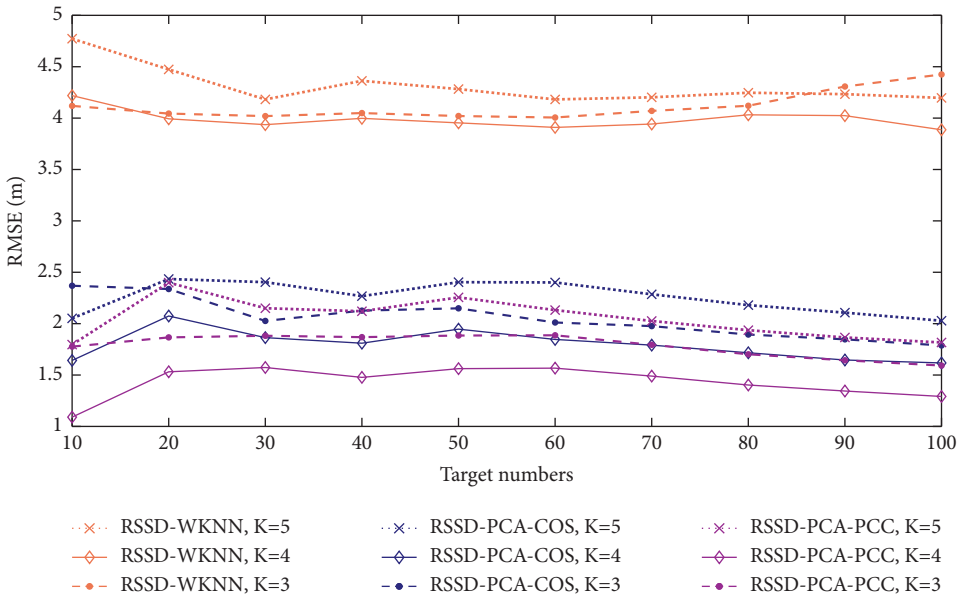

Figure 8: RMSE comparisons among RSSD-WKNN, RSSD-PCA-COS, and the proposed RSSD-PCA-PCC when the number of positioning targets changes from 10 to 100 with 2 m grid distance and 4 APs.

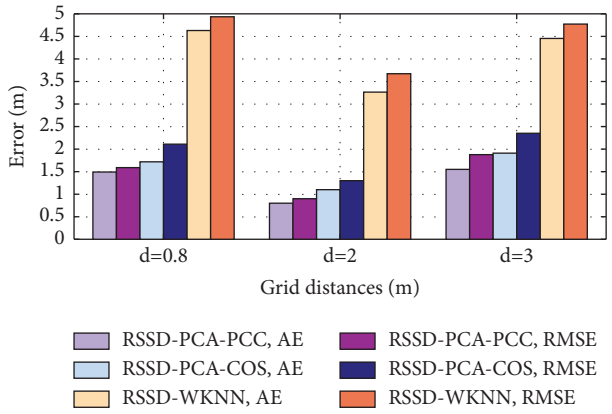

Figure 9: Error comparisons among RSSD-WKNN, RSSD-PCA-COS, and proposed RSSD-PCA-PCC with 0.8 m, 2 m, and 3 m grid distances, 4 APs, and $K = 4$.

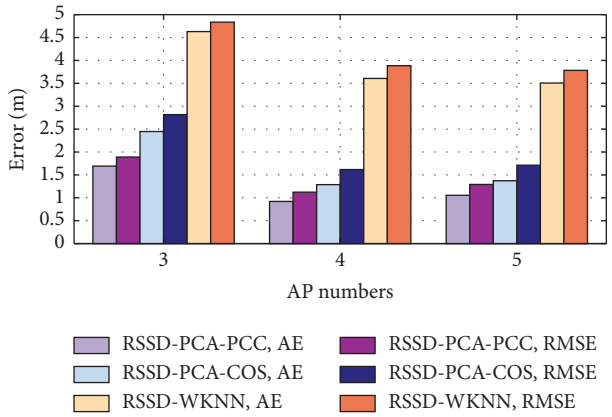

Figure 10: Error comparisons among RSSD-WKNN, RSSD-PCA-COS, and proposed RSSD-PCA-PCC with 3 APs, 4 APs, 5 APs, 2 m grid distance, and $K = 4$.

Table 5: Computational complexity comparison of different algorithms.

Algorithm	Average positioning error (m)	Running time (s)
RSSD-WKNN	3.607	0.653
RSSD-PCA-COS	1.288	0.386
RSSD-PCA-PCC	1.055	0.273

5. Conclusions

A RSSD-PCA-PCC positioning algorithm for the URE was proposed in this article. The RSSD was chosen as the fingerprint without considering the transmitting power and frequency of the URE. However, the high dimension and redundancy of conventional databases increase the computational complexity and result in incorrect positioning matching in the online stage. To achieve information reorganization and dimension reduction, our approach reconstructed the RSSD fingerprint database with a transformed signal space using PCA. The RSSD-based principal component database was processed by the SVD method to reduce the online computational complexity. In addition, a matching PCC-based method was applied to measure the relative distance of the principal component databases between offline and online stages. The superiority of the proposed RSSD-PCA-PCC algorithm was demonstrated under different selected RP numbers, grid distances, and AP numbers. The probability of the average positioning error within 0.9 m can maintain 52%. And the results verify that the proposed algorithm can reduce the average positioning error by 10% compared with the RSSD-PCA-COS algorithms. In the future, the multi-URE indoor positioning algorithm can be considered to meet the application requirements in different scenarios.

Data Availability

The data used to support the findings of this study are available from the corresponding author upon request.

Conflicts of Interest

The authors declare that there are no conflicts of interest.

Acknowledgments

This research was funded by the Tianjin Municipal Education Commission Scientific Research Program Project (Natural Science) (grant no. 2020KJ057).

References

[1] X. S. Guo, N. Ansari, F. Z. Hu, Y. Shao, N. R. Elikplim, and L. Li, "A survey on fusion-based indoor positioning," *IEEE Communications Surveys & Tutorials*, vol. 22, no. 1, pp. 566–594, 2020.

[2] H. Obeidat, W. Shuaieb, O. Obeidat, and R. Abd-Alhameed, "A review of indoor localization techniques and wireless technologies," *Wireless Personal Communications*, vol. 119, no. 1, pp. 289–327, 2021.

[3] F. Liu, J. Liu, Y. Q. Yin et al., "Survey on WiFi-based indoor positioning techniques," *IET Communications*, vol. 14, no. 9, pp. 1372–1383, 2020.

[4] R. Wazirali, "A review on privacy preservation of location-based services in internet of things," *Intelligent Automation & Soft Computing*, vol. 31, no. 2, pp. 767–779, 2022.

[5] P. A. Zandbergen and S. J. Barbeau, "Positional accuracy of assisted GPS data from high-sensitivityGPS-enabled mobile phones," *Journal of Navigation*, vol. 64, no. 3, pp. 381–399, 2011.

[6] L. Chen, K. Zhang, X. W. Zhu, Y. B. Huang, G. Ou, and H. C. Liu, "Beidou satellites assistant determination by receiving other GNSS downlink signals," *International Journal of Antennas and Propagation*, vol. 2016, Article ID 1413401, 10 pages, 2016.

[7] X. W. Wang, Q. Dang, J. L. Guo, and H. B. Ge, "RFID application of smart grid for asset management," *International Journal of Antennas and Propagation*, vol. 2013, Article ID 264671, 6 pages, 2013.

[8] J. Kunhoth, A. Karkar, S. Al-Maadeed, and A. Al-Ali, "Indoor positioning and wayfinding systems: a survey," *Human-Centric Computing and Information Sciences*, vol. 10, no. 1, pp. 18–41, 2020.

[9] M. Shalaby, M. Shokair, and N. W. Messiha, "Performance enhancement of TOA localized wireless sensor networks," *Wireless Personal Communications*, vol. 95, no. 4, pp. 4667–4679, 2017.

[10] S. Cao, X. Chen, X. Zhang, and X. Chen, "Combined weighted method for TDOA-based localization," *IEEE Transactions on Instrumentation and Measurement*, vol. 69, no. 5, pp. 1962–1971, 2020.

[11] L. Bras, N. B. Carvalho, P. Pinho, L. Kulas, and K. Nyka, "A review of antennas for indoor positioning systems," *International Journal of Antennas and Propagation*, vol. 2012, Article ID 953269, 14 pages, 2012.

[12] G. L. Huang and Y. L. Zhu, "Robust localization in distributed MIMO radar using delay and angle measurements with impulsive noise robust TD/AOA localization in impulsive noise," *International Journal of Antennas and Propagation*, vol. 2021, Article ID 1531234, 12 pages, 2021.

[13] A. Heydari, M. Aghabozorgi, and M. Biguesh, "Optimal sensor placement for source localization based on RSSD," *Wireless Networks*, vol. 26, no. 7, pp. 5151–5162, 2020.

[14] A. K. M. Mahtab Hossain, Y. Y. Jin, W. S. Soh, and H. N. Van, "SSD: a robust RF location fingerprint addressing mobile devices' heterogeneity," *IEEE Transactions on Mobile Computing*, vol. 12, no. 1, pp. 65–77, 2013.

[15] Y. C. Hu and G. Leus, "Robust differential received signal strength-based localization," *IEEE Transactions on Signal Processing*, vol. 65, no. 12, pp. 3261–3276, 2017.

[16] H. Lohrasbipeydeh and T. A. Gulliver, "Robust recursive RSSD based source localization in Gaussian mixture channels," *IEEE Communications Letters*, vol. 24, no. 11, pp. 2498–2502, 2020.

[17] H. Lohrasbipeydeh and T. A. Gulliver, "Improved RSSD-based source localization with unknown sensor position errors," *IEEE Wireless Communications Letters*, vol. 10, no. 9, pp. 1949–1953, 2021.

[18] Y. Y. Zhang, H. F. Wu, X. J. Mei, L. N. Liang, and T. A. Gulliver, "Unknown transmit power RSSD-based localization in a Gaussian mixture channel," *IEEE Sensors Journal*, vol. 22, no. 9, pp. 9114–9123, 2022.

[19] Z. K. Chen, Z. L. Ning, Q. Z. Xiong, and M. S. Obaidat, "A collaborative filtering recommendation-based scheme for WLANs with differentiated access service," *IEEE Systems Journal*, vol. 12, no. 1, pp. 1004–1014, 2018.

[20] R. Zhou, Y. X. Yang, and P. C. Chen, "An RSS transform-based WKNN for indoor positioning," *Sensors*, vol. 21, no. 17, p. 5685, 2021.

[21] A. H. Salamah, M. Tamazin, M. A. Sharkas, and M. Khedr, "An enhanced WiFi indoor localization system based on machine learning," in *Proceedings of the International Conference on Indoor Positioning and Indoor Navigation (IPIN)*, pp. 1–8, IEEE, Alcala de Henares, Spain, October 2016.

[22] S. Liu, R. de Lacerda, and J. Fiorina, "Hierarchical fingerprinting and feature extraction for indoor localization," in *Proceedings of the International Conference on Communications*, Seoul, South Korea, May 2022.

[23] Y. Basiouny, M. Arafa, and A. M. Sarhan, "Enhancing Wi-Fi fingerprinting for indoor positioning system using single multiplicative neuron and PCA algorithm," in *Proceedings of the 12th International Conference on Computer Engineering and Systems (ICCES)*, pp. 295–305, Cairo, Egypt, December 2017.

[24] H. Zhang, Y. L. Liu, and H. Lei, "Localization from incomplete Euclidean distance matrix: performance analysis for the SVD-MDS approach," *IEEE Transactions on Signal Processing*, vol. 67, no. 8, pp. 2196–2209, 2019.

[25] A. Javed, M. Yasir Umair, A. Mirza, A. Wakeel, F. Subhan, and W. Zada Khan, "Position vectors based efficient indoor positioning system," *Computers, Materials & Continua*, vol. 67, no. 2, pp. 1781–1799, 2021.

[26] H. G. Li, M. Trocan, and D. Galayko, "Virtual fingerprint and two-wayranging-based Bluetooth 3D indoor positioning with RSSI difference and distance ratio," *Journal of Electromagnetic Waves and Applications*, vol. 33, no. 16, pp. 2155–2174, 2019.

[27] M. L. Chai, C. G. Li, and H. Huang, "A new indoor positioning algorithm of cellular and wi-fi networks," *Journal of Navigation*, vol. 73, no. 3, pp. 509–529, 2020.

[28] A. Li, J. Fu, H. Shen, and S. Sun, "A cluster principal component analysis based indoor positioning algorithm," *IEEE Internet of Things Journal*, vol. 8, no. 1, pp. 187–196, 2021.

[29] Y. Yang, P. Dai, H. Q. Huang, M. Y. Wang, and Y. J. Kuang, "A semi-simulated RSS fingerprint construction for indoor wi-fi positioning," *Electronics*, vol. 9, no. 10, pp. 1568–1615, 2020.

[30] J. H. Yang, Y. Li, W. Cheng, Y. Liu, and C. X. Liu, "Ekf-gpr-based fingerprint renovation for subset-based indoor localization with adjusted cosine similarity," *Sensors*, vol. 18, no. 1, pp. 318-319, 2018.

[31] G. P. Pochanin, L. Capineri, T. D. Bechtel et al., "Measurement of coordinates for a cylindrical target using times of flight from a 1-transmitter and 4-receiver UWB antenna system," *IEEE Transactions on Geoscience and Remote Sensing*, vol. 58, no. 2, pp. 1363–1372, 2020.

[32] Y. Wu, R. Z. Chen, W. Li, Y. Yu, H. T. Zhou, and K. Yan, "Indoor positioning based on walking-surveyedWi-Fi fingerprint and corner reference trajectory-geomagnetic database," *IEEE Sensors Journal*, vol. 21, no. 17, pp. 18964–18977, 2021.

[33] J. H. Li, X. X. Gao, Z. Y. Hu, H. J. Wang, T. Cao, and L. Yu, "Indoor localization method based on regional division with IFCM," *Electronics*, vol. 8, no. 5, pp. 559–620, 2019.

[34] S. C. Zhang, X. L. Li, M. Zong, X. F. Zhu, and R. L. Wang, "Efficient KNN classification with different numbers of nearest neighbors," *IEEE Transactions on Neural Networks and Learning Systems*, vol. 29, no. 5, pp. 1774–1785, 2018.

[35] C. T. Huang, C. H. Wu, Y. N. Lee, and J. T. Chen, "A novel indoor RSS-based position location algorithm using factor graphs," *IEEE Transactions on Wireless Communications*, vol. 8, no. 6, pp. 3050–3058, 2009.